

DOI:10.1002/ejic.201300751

Electrocatalytic Oxidation of Formate with Nickel Diphosphine Dipeptide Complexes: Effect of Ligands Modified with Amino Acids

Brandon R. Galan,^[a] Matthew L. Reback,^[a] Avijita Jain,^[a] Aaron M. Appel,^{*[a]} and Wendy J. Shaw^{*[a]}

Keywords: Formate / Oxidation / Nickel / Peptide catalysts / Electrocatalysts / Outer coordination sphere / Biocatalysts / Bioinorganic chemistry

A series of nickel bis(diphosphine) complexes with dipeptides appended to the ligands were investigated for the catalytic oxidation of formate to carbon dioxide, a proton, and two electrons. Typical rates of approximately 7 s^{-1} were found, similar to that for the parent complex (ca. 8 s^{-1}), with amino acid size and positioning contributing very little to the rate or operating potential. Hydroxy functionalities did result in lower rates, which were recovered by protecting the hy-

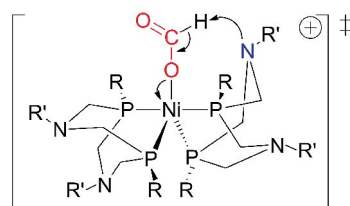
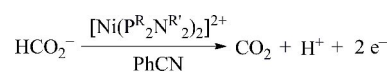
droxy group. The results suggest that the overall dielectric properties introduced by the dipeptides do not play an important role in catalysis, but free hydroxy groups do influence activity, implying contributions from intra- or intermolecular interactions. These observations are important in developing a fundamental understanding of the effect that an enzyme-like outer coordination sphere can have upon molecular catalysts.

Introduction

Given the high global demand for petroleum fuels, research into the development of catalysts for the utilization of alternative carbon-based feedstocks has become an active area of research. In particular, the reduction of carbon dioxide provides an attractive and potentially renewable route to simple carbon-based fuels such as formic acid, carbon monoxide, formaldehyde, methanol, and methane.^[1–7] Of these fuels, formic acid has received considerable attention because of its applications in fuel cell technology and energy storage.^[8–10] As methods of formic acid production for energy storage become more viable, the *electrocatalytic* oxidation of formate as a fuel by using nonprecious metals is critical.

We recently reported that nickel-based electrocatalysts, $[\text{Ni}(\text{P}^{\text{R}}_2\text{N}^{\text{R}'})_2]^{2+}$ with R = Ph (phenyl) or Cy (cyclohexyl) and R' = Ph, 4-MeOPh (methoxyphenyl), Bn (benzyl), or Me (methyl), were well suited for the oxidation of formate with turnover frequencies of up to 15.8 s^{-1} .^[11] Mechanistic studies of this system^[11,12] suggest that after the binding of formate, there is a rate-limiting proton transfer concomitant with a two-electron transfer process accompanied by the loss of CO_2 . This process is thought to involve proton ab-

straction by the pendant amine rather than a direct hydride transfer, because the pendant amines are necessary for catalysis and the rates of catalysis become faster with increasing basicity of the pendant amine (Scheme 1). To date these rates are the highest reported for formate oxidation by homogeneous electrocatalysts and are the only catalysts based on an earth-abundant metal such as nickel.



Scheme 1. Proposed transition state for the electrocatalytic oxidation of formate.^[11,12]

The molybdenum- and iron-containing formate dehydrogenase enzyme ($[\text{Se}]\text{FDH}_\text{H}$), isolated from *E. coli* grown under anaerobic conditions, is capable of interconverting formate and CO_2 at rates of up to 2800 s^{-1} for formate oxidation.^[13] The mechanism proposed for the catalytic system above is analogous to many of the mechanisms proposed for formate dehydrogenase in which two electrons are transferred to the metal in the active site and the proton, H^+ , is transferred to an adjacent heteroatom. The much faster rates for the enzyme in comparison to molecular catalysts

[a] Physical Sciences Division, Pacific Northwest National Laboratory, Richland, WA 99352, USA
E-mail: aaron.appel@pnnl.gov
wendy.shaw@pnnl.gov
<http://www.pnnl.gov>

Supporting information for this article is available on the WWW under <http://dx.doi.org/10.1002/ejic.201300751>.

are likely due in part to the protein scaffold, which can be critical to the function by delivering and removing substrates and products, positioning functional groups to lower the energy level of the transition state, or controlling the polarity of the environment to optimize it for catalysis.^[14–17] We have recently reported that the incorporation of a dipeptide into the outer coordination sphere of these Ni-based electrocatalysts results in rates up to five times faster for the production of hydrogen than that of the parent Ni complex.^[18–20] Amide or acidic/basic amino acid functional groups contribute to the increased rate of hydrogen production. This observation can be best explained by considering that these functional groups help to concentrate water and/or acid near the active site, and they may also aid in proton delivery to the pendant amine;^[18] these are features reminiscent of enzymatic function.

On the basis of the significant rate enhancements observed for hydrogen production catalysis, as well as the potentially large impact that the outer coordination sphere can have on catalysis, the presented studies were undertaken to assess whether similar catalytic enhancements could be observed for formate oxidation. In this work, we examine the influence of a series of known dipeptide catalysts $[\text{Ni}(\text{P}^{\text{Ph}}_2\text{N}^{m/p\text{NNA-R}'_2})_2]^{2+}$ [in which R' is alanine or various amino acid esters] on the electrocatalysis of formate oxidation. The dipeptides consist of a non-natural amino acid, 3-(4-aminophenyl)propionic acid, coupled to the amino acid alanine or to esters of one of the following five amino acids: glycine, alanine, serine, phenylalanine, and tyrosine. We also investigated the positioning of the amino acid functionality by substituting the *para* derivative with the corresponding *meta* derivative of the non-natural amino acid, 3-(3-aminophenyl)propionic acid, as the first amino acid of the dipeptide. The activities of these complexes are discussed in terms of the influence of the outer coordination

sphere on the rates and potentials for the oxidation of formate.

Results

Synthesis and Characterization of Ligands and Complexes

Cyclic diphosphines containing the NNA residues 3-(4-aminophenyl)propionic acid (*para*: *p*-NNA) or 3-(3-aminophenyl)propionic acid (*meta*: *m*-NNA) were prepared with a carboxylic acid termination ($\text{P}^{\text{Ph}}_2\text{N}^{m/p\text{NNA}_2}$) by following previously described protocols.^[18,19] The dipeptide-functionalized ligands, $\text{P}^{\text{Ph}}_2\text{N}^{m/p\text{NNA-R}'_2}$ (Figure 1), were prepared by coupling the amino acid alanine or the amino acid esters AlaOEt, SerOMe, PheOMe, TyrOMe, or Tyr(*t*Bu)OMe to $\text{P}^{\text{Ph}}_2\text{N}^{m/p\text{NNA}_2}$ with use of standard TBTU/HOBT/DIPEA peptide coupling methods.^[21,22] Nickel complexes were prepared by reacting two equivalents of a dipeptide-functionalized ligand with one equivalent of $[\text{Ni}(\text{MeCN})_6]^{2+}$ in acetonitrile, which resulted in a red solution from which a moderately air-sensitive metal complex was obtained in high yield (70–90%) and high purity. The ligands and their $[\text{Ni}(\text{P}^{\text{Ph}}_2\text{N}^{m/p\text{NNA-R}'_2})_2]^{2+}$ complexes were characterized by ³¹P NMR,^[23] ¹H NMR, and ¹H-TOCSY NMR spectroscopy, mass spectrometry, and elemental analysis; additionally, the metal complexes were characterized electrochemically.^[13,20] All results of the characterization are consistent with the proposed structures and similar to those of other reported complexes of this type.^[11,19,20,24,25] Hereafter, the nickel complexes are referred to by the position and identity of the amino acid or dipeptide substituent: for example *m*-SerOMe refers to the nickel complexes that are substituted off the phenyl ring in the *meta*-position and contain the non-natural amino acid coupled to serine methyl ester.

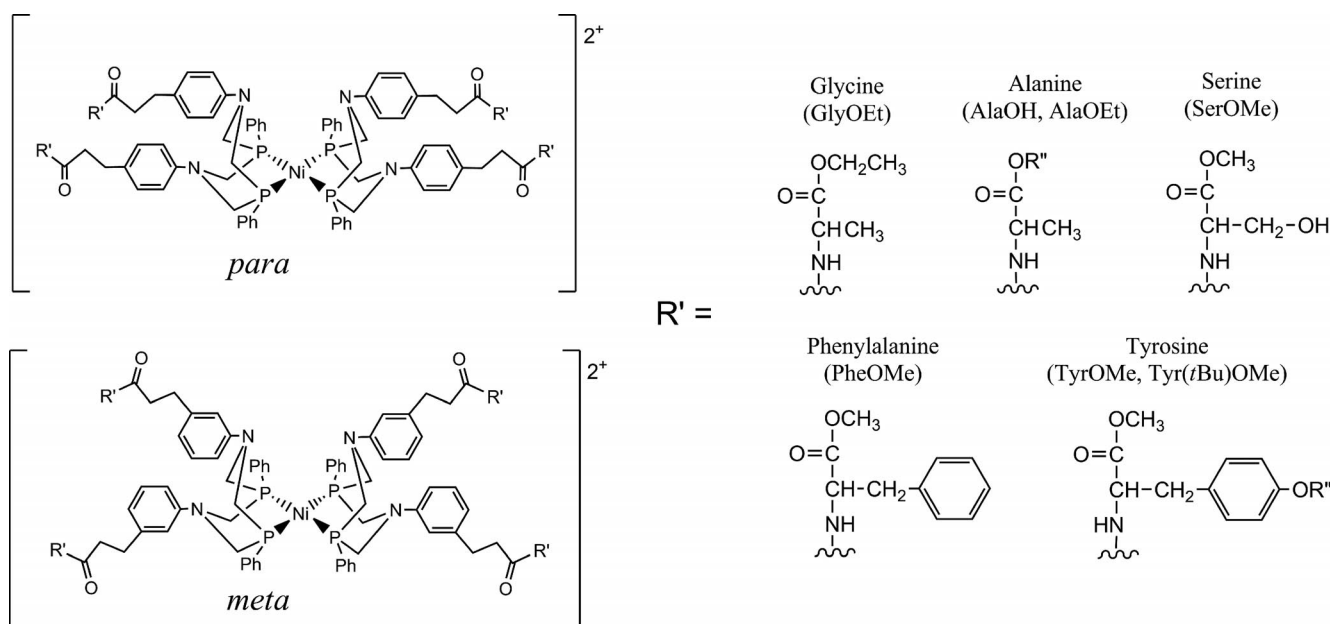


Figure 1. Dipeptide esters investigated in this study (alanine: R'' = H or ethyl, tyrosine: R'' = H or *tert*-butyl).

Electrochemical Studies

As previously reported, each of the dipeptide ester complexes shows two distinct, reversible reduction waves corresponding to the $\text{Ni}^{\text{II/I}}$ and the $\text{Ni}^{\text{I/0}}$ couples (Figure 2).^[18] Differences in redox potentials for all of the complexes are small: $E_{1/2}$ values are within 20 mV for both the $\text{Ni}^{\text{II/I}}$ potentials (−0.83 to −0.85 V) and the $\text{Ni}^{\text{I/0}}$ potentials (−1.03 V to −1.05 V), which indicates that the substituents have minimal impact on the metal center.

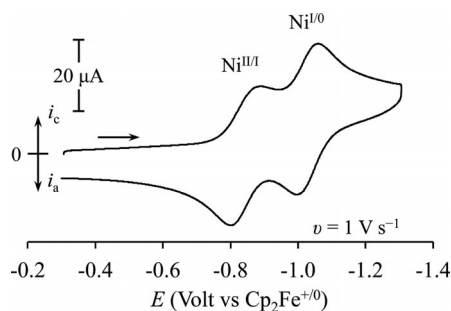


Figure 2. The cyclic voltammogram of *p*-SerOMe is representative of the cyclic voltammograms for each of the complexes reported here.^[18] Conditions: 0.7 mM complex in 0.2 M $\text{Et}_4\text{N}^+\text{BF}_4^-$ acetonitrile solution, glassy carbon working electrode; scan rate 1 V/s. Potentials are referenced to the ferrocenium/ferrocene couple (0.0 V).

Electrochemical Oxidation of Formate

Each of the dipeptide complexes shown in Figure 1 were examined for their activity for the electrochemical oxidation of formate. A representative cyclic voltammogram of *p*-SerOMe as a function of formate concentration in benzonitrile is shown in Figure 3, where benzonitrile was used because of the higher solubility of the Ni^0 complex. The reversible wave at −1.33 V is due to the cobaltocenium/cobaltocene couple, which was used as an internal standard for catalytic runs. Cobaltocenium hexafluorophosphate $\{\text{CoCp}_2(\text{PF}_6)\}$ was used as an internal reference instead of ferrocene

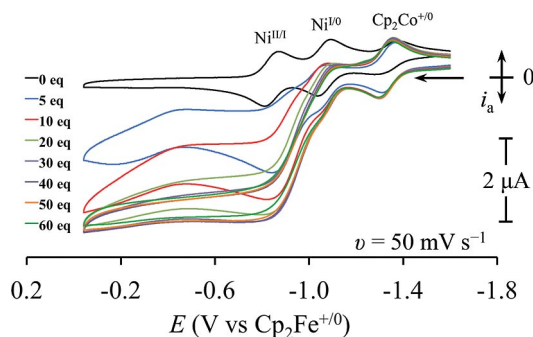


Figure 3. Representative cyclic voltammograms for the addition of formate to any of the dipeptide complexes (shown for *p*-SerOMe), which results in current enhancements consistent with the catalytic oxidation of formate. Conditions: 1.0 mM catalyst in 0.2 M TBAPF₆ benzonitrile solution, glassy carbon working electrode; scan rate 50 mV/s. Potentials are referenced to the ferrocenium/ferrocene couple (0.0 V) using cobaltocenium/cobaltocene as an internal reference (−1.33 V).

(Cp_2Fe), because the ferrocene/ferrocenium couple overlaps with the catalytic wave observed for formate oxidation. Upon addition of formate (added as $\text{NBu}_4\text{HCO}_2\cdot\text{HCO}_2\text{H}$),^[11] an increase in current (i_{cat}) is observed at the potential of the $\text{Ni}^{\text{II/I}}$ couple (Figure 3), consistent with the catalytic oxidation of formate. This current increases and gradually shifts to more negative potentials as the concentration of formate increases, previously interpreted as a fast following reaction (formate binding) as the Ni^{I} species is oxidized to form Ni^{II} .^[11] This shift occurs at consistently higher formate concentrations for the dipeptide complexes than for the unsubstituted complex, suggesting that the binding of formate is hindered for these bulkier catalysts.

A representative plot of the turnover frequency (TOF) of the catalyst vs. formate concentration reveals similar behavior to that observed for the parent catalyst (Figure 4).^[11] The catalytic reaction was shown to be first order in catalyst (Figure S1), as previously observed for complexes without the dipeptides.^[11] These results suggest that the catalysts that contain dipeptides operate by the same mechanism as those without the dipeptides, for which the rate-determining step at high formate concentration was proposed to be the proton abstraction by the pendant amine concomitant with electron transfer to the metal center.

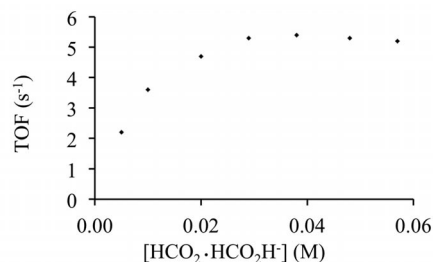


Figure 4. For dipeptide catalysts (shown for *p*-SerOMe), formate oxidation is initially dependent on formate concentration, followed by a region in which it is independent of formate concentration, similar to the parent catalysts. The rates were obtained by using the current in the formate concentration independent region (above 0.03 M).

The current enhancement (i_{cat}/i_p) in the presence of formate substrate can be converted to a catalytic rate (TOF) using Equations (1) and (2). The terms i_{cat} and i_p refer to the current observed in the presence and absence of formate substrate, respectively.

$$\frac{i_{\text{cat}}}{i_p} = \frac{n_{\text{cat}}}{0.4463} \sqrt{\frac{RT}{F\nu n_p^3}} \sqrt{k[\text{HCO}_2^-]^x} \quad (1)$$

$$\text{TOF} = k = \frac{F\nu n_p^3}{RT} \left(\frac{0.4463}{n_{\text{cat}}} \right)^2 \left(\frac{i_{\text{cat}}}{i_p} \right)^2 \quad (2)$$

Equation (1) can be rearranged to yield Equation (2) in the formate-independent region. Equation (2) was used to calculate the TOF for the catalytic oxidation of formate using Faraday's constant (F), the scan rate in V/s (ν), the

number of electrons in the wave in the absence of formate (n_p), the universal gas constant (R), the reaction temperature in Kelvin (T), and the number of electrons involved in the catalytic process (n_{cat}).^[26–28] The calculated rates of formate oxidation are presented in Table 1 and range from unobserved (p -AlaOH) up to 8.5 s^{-1} (m -GlyOMe), with an average of 6.1 s^{-1} . Little difference was observed as a function of amino acid ester identity, and typically, the *meta*-substituted complexes were slightly faster than the *para*-substituted complexes. Notably, m/p -TyrOMe both had significantly lower TOFs than the other complexes, prompting the investigation of the m/p -Tyr(*t*Bu)OMe. The alkylation of these complexes resulted in an increase in the catalytic TOF to the same range as the other dipeptide-containing complexes, as shown in Table 1.

Table 1. TOF values for the electrocatalytic oxidation of formate with dipeptide-substituted catalysts.

Entry ^[a]	Catalyst (R')	TOF [s ⁻¹]	Entry ^[a]	Catalyst (R')	TOF [s ⁻¹]
1 ^[11]	P ^{Ph} ₂ N ^{Ph} ₂	7.4 ± 0.7	8	<i>p</i> -PheOMe	6.0 ± 0.9
2	<i>p</i> -GlyOEt	7.5 ± 0.4	9	<i>m</i> -PheOMe	6.8 ± 0.9
3 ^[b]	<i>m</i> -GlyOEt	8.5 ± 0.3	10	<i>p</i> -TyrOMe	3.3 ± 0.4
4	<i>p</i> -AlaOEt	6.2 ± 1	11	<i>m</i> -TyrOMe	1.8 ± 0.4
5	<i>m</i> -AlaOEt	7.3 ± 1	12	<i>p</i> -Tyr(<i>t</i> Bu)OMe	6.2 ± 0.1
6	<i>p</i> -SerOMe	4.6 ± 1	12	<i>m</i> -Tyr(<i>t</i> Bu)OMe	7.7 ± 1.7
7	<i>m</i> -SerOMe	6.1 ± 0.5	14	<i>p</i> -AlaOH	–

[a] Catalyst (1.0 mM) in a benzonitrile solution of TBAPF₆ (0.2 M); scan rate 50 mV/s. Average of three runs. [b] Average of two runs.

Discussion

It has become widely acknowledged that the outer coordination sphere is intimately involved with the catalytic function of metalloenzymes by providing catalytic control, speed, and efficiency unparalleled by small synthetic biomimetics.^[15,17] If these advantages are to be incorporated into synthetic biomimetics, understanding and predicting how variations in the outer coordination sphere influence catalysis will be essential. The outer coordination sphere is currently not well understood in molecular catalysts, and the dipeptide derivatives studied here provide a foundation for developing predictive tools. The overall observation in comparing the rates of formate oxidation with dipeptide-substituted complexes is that there is very little change, regardless of size or substitution position, when compared to the unmodified complex, Ni(P^{Ph}₂N^{Ph}₂)₂²⁺ (TOF = 8 s^{-1}).^[11] The exceptions to this pattern are the polar-substituted complexes, *m*- and *p*-TyrOMe, which are four times slower than the unmodified catalyst, the *p*-SerOMe, which is two times slower, and the unprotected *p*-AlaOH which was not catalytic. It is tempting to conclude that the difference for these catalysts is related to size; however, it is clear that size is not the key factor, since Phe and Tyr are essentially the same size but m/p -TyrOMe is 2–4 times slower than m/p -PheOMe. Furthermore, *p*-PheOMe performs as well as the smaller *p*-GlyOEt and *p*-AlaOEt derivatives, suggesting little influence of the change in the sterics of the dipeptides.

The lower catalytic activity for the TyrOMe derivatives may be the result of the free phenol residue present in the complexes. To test this hypothesis, *meta*- and *para*-substituted catalyst derivatives were synthesized, with the phenol protected as the *tert*-butyl ether to yield m/p -Tyr(*t*Bu)OMe. This protected complex performed similarly to the other complexes that were studied ($6\text{--}8\text{ s}^{-1}$) under identical reaction conditions, suggesting that the unprotected phenol group is indeed responsible for the reduction in rates. It is not expected that the deprotonated substrate, formate, would be able to appreciably deprotonate the phenol dipeptides in TyrOMe, since the pK_a of formic acid (which has not been reported in MeCN to the best of our knowledge) is expected to be similar to the pK_a of acetic acid, 23.5,^[29] and the pK_a of phenol in acetonitrile, 29.1,^[30] is considerably higher than the expected value for formic acid. A possible explanation for the role of the phenol group is intra- or intermolecular interactions that result in a change in ligand dynamics or an electronic effect. These may be due to strong hydrogen-bonding interactions, possibly with either formate or another phenol group. Regardless of the precise cause, the presence of the protic group results in lower rates than those for analogous complexes without this functionality.

A similar mechanism may also be responsible for the decreased rate observed for *p*-SerOMe and the loss of catalytic activity observed for the acidic amino acid complex, *p*-AlaOH. Previous studies have shown restricted motion in the five-coordinate (solvent bound) *p*-Ala-OH complex, best described by reduced structural interconversion of axial and equatorial phosphine groups due to intra- or intermolecular interactions for this complex.^[20] Consequently, the decrease in activity could also be related to intra- or intermolecular interactions that limit either formate association or essential ligand flexibility such as chair/boat interconversions.

The use of polar and aromatic side chains such as tyrosine has been shown to assist in tuning active sites in enzymes.^[15,17] Additionally, the global dielectric constant of the outer coordination sphere will change as a result of the OH groups. However, the formate oxidation catalysts studied here had very little enhancement from the outer coordination sphere. We previously demonstrated that this series of catalysts had a significant impact on hydrogen production.^[18–20] The catalyst activities ranged over almost an order of magnitude, the fastest catalysts operating five times faster than the unmodified catalysts. In that case, the increase in activity was interpreted to be due to the ability to concentrate water and protons near the active site. In the case of formate oxidation, the rate-limiting step is proposed to be an intramolecular proton-coupled electron transfer,^[11,12] and therefore concentrating protons is not expected to enhance the rate. The expected effect would have been due to the contributions of polar or aromatic groups altering the electronic environment near the active site or contributing to lower the energy barrier of the transition state. These effects were also not observed here, suggesting that the global dielectric properties around the active site

are not important in the $\text{Ni}(\text{P}^{\text{R}}_2\text{N}^{\text{R}'_2})_2$ series of catalysts for the oxidation of formate. Changes in local dielectric constant close to the metal center and substrate may have greater influence, and studies with positioned functional groups are underway.

Summary and Conclusions

A series of dipeptide-substituted catalysts shows activity for the oxidation of formate, and changing the amino acid functional groups, size, or positioning had little influence on the catalytic rates. Therefore, the global dielectric properties do not appear to affect the activity of these complexes; however, the presence of protic groups did inhibit catalysis, possibly due to intra- or intermolecular interactions limiting ligand dynamics. This work provides additional insight into the role of a flexible outer coordination sphere on $\text{Ni}(\text{P}^{\text{R}}_2\text{N}^{\text{R}'_2})_2^{2+}$ molecular catalysts and provides a starting point for introducing and evaluating a positioned outer coordination sphere.

Experimental Section

Materials and Methods

All reactions were performed under an inert atmosphere of nitrogen by using standard Schlenk techniques or in a glovebox. Solvents were de-oxygenated and purified with an Innovative Technology, Inc. PureSolv™ solvent purification system. $[\text{D}_3]$ Acetonitrile (Cambridge Isotope Laboratories, 99.5% D) was vacuum-distilled from P_2O_5 . $[\text{D}]$ Chloroform (Cambridge Isotope Laboratories, 99.5% D) was degassed and stored over molecular sieves. Water was dispensed from a Millipore MilliQ purifier at 18 M Ω and sparged with nitrogen. 2-(1*H*-Benzotriazole-1-yl)-1,1,3,3-tetramethyluronium tetrafluoroborate (TBTU), 3-(4-aminophenyl)propionic acid, 3-(3-aminophenyl)propionic acid, ammonium chloride, and trimethylsilyl chloride (Aldrich) were used as received. Diisopropylethylamine (DIPEA) (Aldrich) was degassed prior to use by the freeze-pump-thaw method. The amino acid esters were purchased from Nova Biochem or Sigma Aldrich and used as received. $[\text{Ni}(\text{MeCN})_6](\text{BF}_4)_2$ and $\text{P}^{\text{Ph}_2}\text{N}^{\text{P}^{\text{R}}_2\text{N}^{\text{R}'_2}}_2$ [p -NNA = 3-(4-aminophenyl)propionic acid and m -NNA = 3-(3-aminophenyl)propionic acid] were prepared by following literature methods.^[18,31,32] All ligands and metal complexes were prepared as previously reported, similar to the preparations for the Tyr(*t*Bu)OMe ligands and complexes reported below.^[18]

$\text{P}^{\text{Ph}_2}\text{N}^{\text{P}^{\text{R}}_2\text{N}^{\text{R}'_2}}_2\text{-Tyr}(\text{tBu})\text{OMe}_2$ [Tyr(*t*Bu)OMe = *O*-*tert*-Butyl-L-Tyrosine Methyl Ester]: TBTU (2.0 equiv., 107.0 mg, 0.33 mmol) and HOBT (2.0 equiv., 45.0 mg, 0.33 mmol) were added to a dichloromethane solution containing $\text{P}^{\text{Ph}_2}\text{N}^{\text{P}^{\text{R}}_2\text{N}^{\text{R}'_2}}_2$ (1.0 equiv., 100.0 mg, 0.17 mmol) and DIPEA (2.2 equiv., 47.4 mg, 63.9 μL 0.38 mmol). The mixture was stirred for 20 min and then *O*-*tert*-butyl-L-tyrosine methyl ester hydrochloride (2.0 equiv., 96.0 mg, 0.33 mmol) was added and stirred overnight. The solution was extracted with water to remove residual chloride, and the dichloromethane solution was dried under vacuum to yield a yellow viscous oil. This product was then redissolved in a minimal amount of dichloromethane and flash precipitated from diethyl ether. This was repeated three more times. The resulting off-white solid was collected and dried in vacuo. (Yield: 29.6 mg, 0.03 mmol, 32.2%). $^31\text{P}\{^1\text{H}\}$ NMR (CDCl_3): δ =

−49.83 (s) ppm. ^1H NMR (CDCl_3): δ = 7.60–6.65 (m, 26 H, *Ar*), 5.82 [d, 2 H, C(O)NH], 4.83 (m, 2 H, αCH), 4.45 (m, 4 H, PCH_2N), 4.01 (m, 4 H, PCH_2N), 3.61 (s, 6 H, COOCH_3), 3.01 (d, 4 H, βCH_2), 2.80 [m, 4 H, $\text{CH}_2\text{C}(\text{O})\text{N}$], 2.42 (m, 4 H, N-Ph CH_2), 1.32 [s, 18H C(CH_3) $_3$] ppm.

$\text{P}^{\text{Ph}_2}\text{N}^{\text{P}^{\text{R}}_2\text{N}^{\text{R}'_2}}_2\text{-Tyr}(\text{tBu})\text{OMe}_2$ [Tyr(*t*Bu)OMe = *O*-*tert*-Butyl-L-Tyrosine Methyl Ester]: This complex was prepared in an analogous manner to the synthesis described for $\text{P}^{\text{Ph}_2}\text{N}^{\text{P}^{\text{R}}_2\text{N}^{\text{R}'_2}}_2\text{-Tyr}(\text{tBu})\text{OMe}_2$ with the following amounts: TBTU (2.0 equiv., 192.0 mg, 0.60 mmol) and HOBT (2.0 equiv., 81.1 mg, 0.60 mmol) were added to a dichloromethane solution containing $\text{P}^{\text{Ph}_2}\text{N}^{\text{P}^{\text{R}}_2\text{N}^{\text{R}'_2}}_2$ (1.0 equiv., 179.0 mg, 0.30 mmol) and DIPEA (2.2 equiv., 85.1 mg, 115 μL 0.66 mmol). The mixture was stirred for 20 min and then *O*-*tert*-butyl-L-tyrosine methyl ester hydrochloride (2.0 equiv., 172.0 mg, 0.60 mmol) was added. (Yield: 80.3 mg, 0.075 mmol, 26%). $^31\text{P}\{^1\text{H}\}$ NMR (CDCl_3): δ = −47.8 (s) ppm. ^1H NMR (CDCl_3): δ = 7.60–6.48 (m, 26 H, *Ar*), 5.78 [d, 2 H, C(O)NH], 4.76 (m, 2 H, αCH), 4.44 (m, 4 H, PCH_2N), 3.99 (dd, 4 H, PCH_2N), 3.63 (s, 6 H, COOCH_3), 2.87 (m, 4 H, βCH_2), 2.80 [m, 4 H, $\text{CH}_2\text{C}(\text{O})\text{N}$], 2.40 (m, 4 H, N-Ph CH_2), 1.30 [s, 18H C(CH_3) $_3$] ppm.

$\text{Ni}(\text{P}^{\text{Ph}_2}\text{N}^{\text{P}^{\text{R}}_2\text{N}^{\text{R}'_2}}_2\text{-Tyr}(\text{tBu})\text{OMe}_2)_2$ (BF_4) $_2$ [Tyr(*t*Bu)OMe = *O*-*tert*-Butyl-L-Tyrosine Methyl Ester]: The purified $\text{P}^{\text{Ph}_2}\text{N}^{\text{P}^{\text{R}}_2\text{N}^{\text{R}'_2}}_2\text{-Tyr}(\text{tBu})\text{OMe}_2$ ligand (29.6 mg, 0.03 mmol) was added to an acetonitrile solution containing $[\text{Ni}(\text{CH}_3\text{CN})_6](\text{BF}_4)_2$ (0.5 equiv., 7.19 mg, 0.015 mmol) and stirred for 24 h. The resulting red solution was filtered through Celite, and the solvent was removed under vacuum. The residual red oil was then dissolved in a minimal amount of acetonitrile (ca. 2 mL) and added dropwise to 0 °C diethyl ether with stirring until all of the solid had precipitated out of the acetonitrile/diethyl ether solution. The resulting red solid was collected by filtration, washed with diethyl ether, and dried in vacuo. (Yield: 20.1 mg, 8.8 μmol , 56.8%). $^31\text{P}\{^1\text{H}\}$ NMR (CD_3CN): δ = 5.2 (s) ppm. ^1H NMR (CD_3CN): δ = 7.40–6.83 (m, 52 H, *Ar*), 6.68 [d, 4 H, C(O)NH], 4.55 (m, 4 H, αCH), 4.15 (m, 8 H, PCH_2N), 3.82 (m, 8 H, PCH_2N), 3.53 (s, 12 H, COOCH_3), 2.95 (m, 4 H, $\beta\text{CH}_2\text{A}$), 2.83 (m, 4 H, $\beta\text{CH}_2\text{B}$), 2.80 [m, 8 H, $\text{CH}_2\text{C}(\text{O})\text{N}$], 2.42 (m, 8 H, N-Ph CH_2), 1.22 [s, 36 H, C(CH_3) $_3$] ppm. MALDI MS: calcd. for $[\text{Ni}(\text{P}^{\text{Ph}_2}\text{N}^{\text{P}^{\text{R}}_2\text{N}^{\text{R}'_2}}_2\text{-Tyr}(\text{tBu})\text{OMe}_2)_2]^{2+}$ 2186.93; found 2187.24.

$\text{Ni}(\text{P}^{\text{Ph}_2}\text{N}^{\text{P}^{\text{R}}_2\text{N}^{\text{R}'_2}}_2\text{-Tyr}(\text{tBu})\text{OMe}_2)_2$ (BF_4) $_2$ [Tyr(*t*Bu)OMe = *O*-*tert*-Butyl-L-Tyrosine Methyl Ester]: This complex was prepared in an analogous manner to the synthesis described for $[\text{Ni}(\text{P}^{\text{Ph}_2}\text{N}^{\text{P}^{\text{R}}_2\text{N}^{\text{R}'_2}}_2\text{-Tyr}(\text{tBu})\text{OMe}_2)_2](\text{BF}_4)_2$ by using $[\text{Ni}(\text{MeCN})_6](\text{BF}_4)_2$ (0.5 equiv., 18.1 mg, 0.035 mmol) and $\text{P}^{\text{Ph}_2}\text{N}^{\text{P}^{\text{R}}_2\text{N}^{\text{R}'_2}}_2\text{-Tyr}(\text{tBu})\text{OMe}_2$ (1.0 equiv., 78.7 mg, 0.07 mmol). (Yield: 48.2 mg, 24.7 μmol , 58%). $^31\text{P}\{^1\text{H}\}$ NMR (CD_3CN): δ = 4.5 (s) ppm. ^1H NMR (CD_3CN): δ = 7.41–6.83 (m, 52 H, *Ar*), 6.63 [d, 4 H, C(O)NH], 4.51 (m, 4 H, αCH), 4.19 (m, 8 H, PCH_2N), 3.88 (m, 8 H, PCH_2N), 3.54 (s, 12 H, COOCH_3), 2.98 (m, 4 H, $\beta\text{CH}_2\text{A}$), 2.93 (m, 4 H, $\beta\text{CH}_2\text{B}$), 2.83 [m, 8 H, $\text{CH}_2\text{C}(\text{O})\text{N}$], 2.43 (m, 8 H, N-Ph CH_2), 1.24 [s, 36 H, C(CH_3) $_3$] ppm. MALDI MS: calcd. for $[\text{Ni}(\text{P}^{\text{Ph}_2}\text{N}^{\text{P}^{\text{R}}_2\text{N}^{\text{R}'_2}}_2\text{-Tyr}(\text{tBu})\text{OMe}_2)_2]^{2+}$ 2186.93; found 2187.20.

Electrochemistry: All electrochemical experiments were carried out in a glovebox under a nitrogen atmosphere by using a CH Instruments 600 or 1100 series three-electrode potentiostat. The working electrode was a glassy carbon disk (1 mm diameter), and the counter electrode was a glassy carbon rod. A silver wire in electrolyte solution was separated from the working compartment by a Vycor frit (4 mm, BAS) and was used as a pseudo-reference electrode. All potentials were measured by using Cp_2Fe (0 V) or Cp_2Co^+ (−1.33 V) as internal references and all potentials are reported vs. the $\text{Cp}_2\text{Fe}^{+/0}$ couple. All catalyst and $\text{NBu}_4\text{HCO}_2\cdot\text{HCO}_2\text{H}$ solutions^[4] were freshly prepared in a tetra-

butylammonium hexafluorophosphate (TBAPF₆) solution (0.2 M) in benzonitrile prior to analysis.

General Procedure for Electrocatalytic Formate Oxidation (Order with Respect to Formate): In a glovebox, a stock solution of catalyst (1.0 mM) was prepared by dissolving the catalyst in a 5.0 mL volumetric flask with a benzonitrile solution of TBAPF₆ (0.2 M). A 1.0 mL aliquot of the catalyst solution was titrated with aliquots of NBu₄HCO₂·HCO₂H solution in 5 μL increments and cyclic voltammograms were recorded to determine catalytic currents. Plots of TOF vs. [NBu₄HCO₂·HCO₂H] were used to determine the order with respect to formate. The peak current (*i*_p) is the observed current for the Ni^{II/I} couple in the absence of formate. The catalytic current (*i*_{cat}) is the observed peak current in the presence of formate.

Supporting Information (see footnote on the first page of this article): Order with respect to formate; order with respect to catalyst.

Acknowledgments

This work was funded by the US Department of Energy (DOE) Office of Basic Energy Sciences, Division of Chemical Sciences, Geosciences & Biosciences. Pacific Northwest National Laboratory (PNNL) is a multiprogram national laboratory operated for DOE by Battelle.

- [1] E. E. Benson, C. P. Kubiak, A. J. Sathrum, J. M. Smieja, *Chem. Soc. Rev.* **2009**, *38*, 89.
- [2] T. R. Cook, D. K. Dogutan, S. Y. Reece, Y. Surendranath, T. S. Teets, D. G. Nocera, *Chem. Rev.* **2010**, *110*, 6474.
- [3] C. Costentin, M. Robert, J.-M. Saveant, *Chem. Soc. Rev.* **2013**, *42*, 2423.
- [4] J. L. Inglis, B. J. MacLean, M. T. Pryce, J. G. Vos, *Coord. Chem. Rev.* **2012**, *256*, 2571.
- [5] G. A. Olah, G. K. S. Prakash, A. Goepfert, *J. Am. Chem. Soc.* **2011**, *133*, 12881.
- [6] W. Wang, S. Wang, X. Ma, J. Gong, *Chem. Soc. Rev.* **2011**, *40*, 3703.
- [7] C. D. Windle, R. N. Perutz, *Coord. Chem. Rev.* **2012**, *256*, 2562.
- [8] C. Rice, S. Ha, R. I. Masel, A. Wieckowski, *J. Power Sources* **2003**, *115*, 229.
- [9] C. Song, *Catal. Today* **2002**, *77*, 17.
- [10] Y. Zhu, S. Y. Ha, R. I. Masel, *J. Power Sources* **2004**, *130*, 8.
- [11] B. R. Galan, J. Schoffel, J. C. Linehan, C. Seu, A. M. Appel, J. A. S. Roberts, M. L. Helm, U. J. Kilgore, J. Y. Yang, D. L. DuBois, C. P. Kubiak, *J. Am. Chem. Soc.* **2011**, *133*, 12767.
- [12] C. S. Seu, A. M. Appel, M. D. Doud, D. L. DuBois, C. P. Kubiak, *Energy Environ. Sci.* **2012**, *5*, 6480.
- [13] M. J. Axley, A. Böck, T. C. Stadtman, *Proc. Natl. Acad. Sci. USA* **1991**, *88*, 8450.
- [14] T. E. Creighton, *Proteins*; W. H. Freeman and Company: New York, **1996**.
- [15] S. W. Ragsdale, *Chem. Rev.* **2006**, *106*, 3317.
- [16] J. Lee, N. M. Goodey, *Chem. Rev.* **2011**, *111*, 7595.
- [17] S. Karlin, Z. Y. Zhu, K. D. Karlin, *Proc. Natl. Acad. Sci. USA* **1997**, *94*, 14225.
- [18] M. L. Reback, B. Ginovska-Pangovska, M.-H. Ho, A. Jain, T. C. Squier, S. Rauegi, J. A. S. Roberts, W. J. Shaw, *Chem. Eur. J.* **2013**, *19*, 1928.
- [19] A. Jain, S. Lense, J. C. Linehan, S. Rauegi, H. Cho, D. L. DuBois, W. J. Shaw, *Inorg. Chem.* **2011**, *50*, 4073.
- [20] A. Jain, M. L. Reback, M. L. Lindstrom, C. E. Thogerson, M. L. Helm, A. M. Appel, W. J. Shaw, *Inorg. Chem.* **2012**, *51*, 6592.
- [21] S. Balalaie, M. Mahdidoust, R. Eshaghi-Najafabadi, *J. Iraqi Chem. Soc.* **2007**, *4*, 364.
- [22] A. El-Faham, F. Albericio, *Chem. Rev.* **2011**, *111*, 6557.
- [23] R. W. Alder, P. R. Allen, M. Murray, A. G. Orpen, *Angew. Chem.* **1996**, *108*, 1211; *Angew. Chem. Int. Ed. Engl.* **1996**, *35*, 1121.
- [24] U. J. Kilgore, M. P. Stewart, M. L. Helm, W. G. Dougherty, W. S. Kassel, M. Rakowski DuBois, D. L. DuBois, R. M. Bullcock, *Inorg. Chem.* **2011**, *50*, 10908.
- [25] A. D. Wilson, R. H. Newell, M. J. McNevin, J. T. Muckerman, D. M. Rakowski, D. L. DuBois, *J. Am. Chem. Soc.* **2006**, *128*, 358.
- [26] R. S. Nicholson, I. Shain, *Anal. Chem.* **1964**, *36*, 706.
- [27] J. M. Saveant, E. Vianello, *Electrochim. Acta* **1967**, *12*, 629.
- [28] J. M. Saveant, E. Vianello, *Electrochim. Acta* **1965**, *10*, 905.
- [29] A. Kütt, I. Leito, I. Kaljurand, L. Sooväli, V. M. Vlasov, L. M. Yagupolskii, I. A. Koppel, *J. Org. Chem.* **2006**, *71*, 2829.
- [30] A. Kütt, V. Movchun, T. Rodima, T. Dansauer, E. B. Rusanov, I. Leito, I. Kaljurand, J. Koppel, V. Pihl, I. Koppel, G. Ovsjanikov, L. Toom, M. Mishima, M. Medebielle, E. Lork, G.-V. Rosenthaler, I. A. Koppel, A. A. Kolomeitsev, *J. Org. Chem.* **2008**, *73*, 2607.
- [31] B. J. Hathaway, D. G. Holah, A. E. Underhill, *J. Chem. Soc.* **1962**, 2444.
- [32] G. A. Le, V. Artero, B. Jousset, P. D. Tran, N. Guillet, R. Metaye, A. Fihri, S. Palacin, M. Fontecave, *Science (Washington, DC, U.S.)* **2009**, *326*, 1384.

Received: June 15, 2013

Published Online: September 3, 2013